Controlling the fluorescence lifetime of a single emitter on the nanoscale using a plasmonic superlens

L. S. Froufe-Pérez[1,2,3] and R. Carminati[1,2,*]

[1]*Laboratoire d'Optique Physique, ESPCI, 10 rue Vauquelin, 75231 Paris Cedex 05, France*

[2]*Laboratoire Photons et Matière, CNRS UPR 5, ESPCI, 10 rue Vauquelin, 75231 Paris Cedex 05, France*

[3]*Instituto de Ciencia de Materiales de Madrid, CSIC, Cantoblanco 28049 Madrid, Spain*

(Received 27 May 2008; published 4 September 2008)

Coupling a single dipole emitter to a metallic nanoparticle through the optical modes of a planar superlens made of left-handed material can lead to substantial modifications of its spontaneous decay rate. We provide a quantitative study based on exact numerical simulation and show that such a scheme could allow the detection, the localization, and the control of the emitter dynamics with nanometer-scale sensitivity, as well as the determination of its transition dipole orientation.

DOI: 10.1103/PhysRevB.78.125403 PACS number(s): 78.67.−n, 78.68.+m, 32.50.+d

I. INTRODUCTION

Since the experiments of Drexhage,[1] it has been known that the fluorescence lifetime of a dipole emitter (e.g., atom, molecule, quantum dot) can be substantially modified close to a metal surface. Lifetime modifications are induced by changes in the local density of electromagnetic modes,[2] and are quantitatively described by the classical electrodynamic response of the surface.[3,4] The development of near-field optics techniques has stimulated the use of metallic tips, nanoparticles or nanostructured substrates to modify the spontaneous emission features (fluorescence lifetime or fluorescence intensity) of single emitters with nanometer-scale sensitivity and with an improving level of control.[5–10] These nanostructures, commonly denoted by nanoantennas, not only modify the spontaneous emission dynamics but also act on the angular radiation pattern.[11–16] New behaviors have also been demonstrated by coupling emitters to thin metallic films. Donors and acceptors have been coupled by fluorescence resonance energy transfer (FRET) through the plasmon modes of silver films with thicknesses up to 120 nm (i.e., far beyond the usual Förster radius).[17] Efficient excitation and detection of the fluorescence of single molecules has been achieved through a gold film, and the role of surface plasmons in the process has been analyzed.[18] At frequencies such that $\mathrm{Re}[\epsilon(\omega)]\simeq -1$, where $\epsilon(\omega)$ is the relative permittivity of the material (corresponding to the plasmon-polariton or phonon-polariton resonance of a flat surface), the near-field coupling of a source to the surface modes of the film allow to enter the so-called "superlens" regime, in which a near-field optical image can be translated to the opposite side of the film with subwavelength resolution. This is true, in principle, for a primary source as in fluorescence emission and for a secondary source as in conventional imaging. Images in the superlens regime have been produced with silver slabs at the plasmon-polariton resonance frequency[19,20] and with a SiC slab at the phonon-polariton resonance frequency.[21] The superlens behavior was originally proposed[22] as the quasistatic limiting case of the perfect lens made of a slab of left-handed (or negative index) material (LHM), i.e., a material with both $\mathrm{Re}[\epsilon(\omega)]=-1$ and $\mathrm{Re}[\mu(\omega)]=-1$, where $\mu(\omega)$ is the relative magnetic permeability. Left-handed materials have received a lot of attention due to their ability to produce negative refraction, leading to the concept of perfect lens.[22,23] Although the fabrication of left-handed metamaterials is a real challenge, negative refraction has been demonstrated at microwave frequencies,[24] and at near-infrared and optical frequencies.[25–27] In terms of image formation with negative-index slabs, absorption drastically reduces the perfect lensing capabilities.[28] Compared to a purely plasmonic system (i.e., a nonmagnetic material with $\mathrm{Re}[\epsilon(\omega)]\simeq -1$), the improvement when using a left-handed material is chiefly due to a better impedance matching, but the coupling mechanism through an absorbing left-handed slab is essentially plasmonic in nature. In the following, we shall denote by "plasmonic superlens" a slab of left-handed material with a non-negligible level of absorption.

In this work, we study theoretically the possibility of using a plasmonic superlens to act on the fluorescence lifetime of an isolated molecule with high sensitivity and nanometer-scale spatial resolution. The concept we propose relies on the coupling of a metallic nanoparticle with a single molecule through a plasmonic superlens. The configuration is similar to that described in Ref. 21 for conventional near-field imaging. The nanoparticle is assumed to be attached, e.g., at the end of a near-field probe. We use quantitative three-dimensional numerical simulations to calculate spontaneous decay-rate modifications induced on the molecule when the nanoparticle scans the opposite side of the plasmonic superlens. We show that this scheme allows the detection, the localization, and the control of the emitter dynamics with nanometer-scale sensitivity, as well as the determination of its transition dipole orientation. Such a geometry is appealing for applications in which the vicinity of the molecule is not directly accessible to a near-field probe (e.g., emitter embedded in the solid substrate of a photonic device, fluorophores in biological media).

II. GEOMETRY AND NUMERICAL METHOD

The geometry is schematically represented in Fig. 1. A single dipole emitter (fluorescent molecule) in its excited state lies below a slab of LHM with width L. At the emission

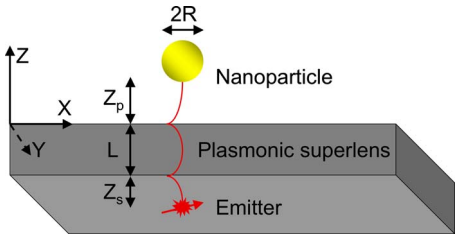

FIG. 1. (Color online) Geometry of the system. A metallic nanoparticle couples to a single emitter through a slab, in a regime where the slab behaves as a plasmonic superlens.

frequency ω of the molecule, the slab is assumed to behave as a plasmonic superlens, such that $\mathrm{Re}[\epsilon(\omega)]=-1$ and $\mathrm{Re}[\mu(\omega)]=-1$, with a non-negligible level of absorption. The distance from the emitter to the slab surface is z_s. A spherical metallic nanoparticle with radius R lies on the opposite side of the slab. The distance from the surface of the nanoparticle to the slab surface is z_p.

In the weak-coupling regime, the spontaneous decay rate Γ of the molecule takes the form[29]

$$\Gamma = \frac{2}{\hbar}|\mathbf{p}|^2 \mathrm{Im}[\mathbf{u}\cdot\mathbf{G}(\mathbf{r},\mathbf{r},\omega)\cdot\mathbf{u}], \tag{1}$$

where $\mathbf{r}$ is the position of the molecule, $\mathbf{p}$ the transition dipole, and $\mathbf{u}$ a unit vector in the direction of $\mathbf{p}$. The dyadic $\mathbf{G}$ is the Green's function of the system, connecting an electric dipole at position $\mathbf{r}$ to the radiated electric field at position $\mathbf{r}'$ through the relation $\mathbf{E}(\mathbf{r}',\omega)=\mathbf{G}(\mathbf{r}',\mathbf{r},\omega)\cdot\mathbf{p}$. In free space, the decay rate is obtained from the vacuum Green's function $\mathbf{G}_0$, and reads $\Gamma_0=\omega^3|\mathbf{p}|^2/(3\pi\epsilon_0\hbar c^3)$. The calculation of the decay rate amounts to calculate the Green's function $\mathbf{G}(\mathbf{r}',\mathbf{r},\omega)=\mathbf{G}_0(\mathbf{r}',\mathbf{r},\omega)+\mathbf{S}(\mathbf{r}',\mathbf{r},\omega)$, where $\mathbf{S}(\mathbf{r}',\mathbf{r},\omega)$ is the modification of the vacuum Green's function induced by the slab-nanoparticle system (for simplicity, we omit the dependence on ω in the fields and Green's functions in the following). Since $\mathbf{G}_0$ is known analytically, we only need to compute the Green's function $\mathbf{S}(\mathbf{r}',\mathbf{r})$. It is deduced from the electric field scattered at a position $\mathbf{r}'$ when the slab-nanoparticle system is illuminated by a classical point dipole placed at a position $\mathbf{r}$: $\mathbf{E}_s(\mathbf{r}')=\mathbf{S}(\mathbf{r}',\mathbf{r})\cdot\mathbf{p}$. In order to compute numerically the Green's function $\mathbf{S}(\mathbf{r}',\mathbf{r})$, we proceed in two steps. First, we calculate the Green's function $\mathbf{S}_{\mathrm{slab}}(\mathbf{r}',\mathbf{r})$ of the isolated slab, which has an analytical expression in Fourier space (angular spectrum representation).[30] The angular spectrum involves Fresnel reflection and transmission factors that account for the properties of the interfaces (in particular surface modes are included in this formalism without any approximation). Second, we use the coupled dipole method[31] to calculate the field scattered by the full system, including far-field and near-field interactions between the slab and the nanoparticle in a self-consistent manner. In this approach, the nanoparticle is meshed in a set of N electric dipoles with polarizability $\alpha(\omega)$. The electromagnetic response of the nanoparticles is described by the polarizability $\alpha(\omega)$ including radiation reaction.[31,32] The correct form of the polarizability is necessary in order to satisfy energy conservation (or the optical theorem). The scattered field at position $\mathbf{r}'$ reads

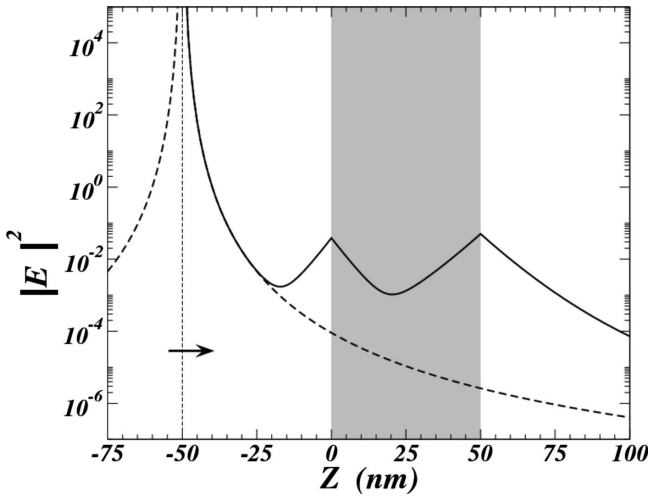

FIG. 2. Solid line: Square modulus of the electric field (arb. units) radiated by a single electric dipole in front of a LHM slab with relative permittivity $\varepsilon=-1+0.01i$ and relative permeability $\mu=-1+0.01i$. The slab lies between $z=0$ and $z=50$ nm (indicated by the gray region). The dipole is oriented along the z direction and is placed at $z_s=-50$ nm (indicated by the arrow). Dashed line: same calculation in absence of the slab.

$$\mathbf{E}_s(\mathbf{r}') = \mathbf{S}_{\mathrm{slab}}(\mathbf{r}',\mathbf{r})\cdot\mathbf{p} + \alpha(\omega)\epsilon_0 \times \sum_{j=1,N} [\mathbf{G}_0(\mathbf{r}',\mathbf{r}_j) + \mathbf{S}_{\mathrm{slab}}(\mathbf{r}',\mathbf{r}_j)]\cdot\mathbf{E}_{\mathrm{exc},j}, \tag{2}$$

where $\mathbf{r}_j$ is the position and $\mathbf{E}_{\mathrm{exc},j}$ the exciting field of dipole number j. The exciting field can be written in a self-consistent manner:

$$\mathbf{E}_{\mathrm{exc},j} = [\mathbf{G}_0(\mathbf{r}',\mathbf{r}) + \mathbf{S}_{\mathrm{slab}}(\mathbf{r}',\mathbf{r})]\cdot\mathbf{p} + \alpha(\omega)\epsilon_0 \times \sum_{j\neq k} [\mathbf{G}_0(\mathbf{r}_j,\mathbf{r}_k) + \mathbf{S}_{\mathrm{slab}}(\mathbf{r}_j,\mathbf{r}_k)]\cdot\mathbf{E}_{\mathrm{exc},k} + \alpha(\omega)\epsilon_0\mathbf{S}_{\mathrm{slab}}(\mathbf{r}_j,\mathbf{r}_j)\mathbf{E}_{\mathrm{exc},j}. \tag{3}$$

Writing Eq. (3) for each dipole leads to a linear system of N equations, which is solved numerically. Once the exciting field of each dipole of the mesh is known, Eq. (2) is used to compute the scattered field at any position. In the context of single-molecule fluorescence, the coupled dipole method is attractive because it permits calculation of Green's functions in a natural way and is well-suited to the study of complex three-dimensional geometries, including disordered systems.[33,34]

III. COUPLING MECHANISM

In order to identify the coupling mechanism between the molecule and the nanoparticle, we have calculated the field emitted by a classical electric dipole placed at the position of the molecule, in the presence of the slab alone [this amounts to calculate the Green's function $\mathbf{S}_{\mathrm{slab}}(\mathbf{r}',\mathbf{r})$]. We show in Fig. 2 the square modulus of the electric field along a line

perpendicular to the slab, passing through the location of the molecule. The orientation of the transition dipole is perpendicular to the slab surfaces (the molecule position is indicated by the vertical dotted line in Fig. 2, its orientation being indicated by the arrow). The solid line is the calculation in the presence of the slab; the dashed line is the same calculation in vacuum.

The field structure exhibits spatial variations characteristic of a coupling to the surface modes of a thin film. The emitter couples evanescently to the slab on the left-hand side. The internal structure of the field shows that it is built by evanescent coupling of the surface modes of the isolated interfaces. An important consequence is that the field intensity at $z=100$ nm in vacuum (i.e., at 50 nm from the right-hand side interface) is about 15 times higher than it would be in absence of the slab. In these conditions, the coupling between the molecule and an object placed on the opposite side of the slab is expected to be enhanced, as we shall demonstrate below. Finally, we stress that the field structure across the superlens is similar to the structure that would be obtained on a purely metallic thin film excited at plasmon resonance.[35] The main difference when using a left-handed material is that the impedance matching is increased so that the transmitted intensity is larger. This also means that the coupling we will discuss below between the molecule and a nanoparticle bear strong similarity with the long-range FRET coupling that has been discussed in Ref. 17 with a purely metallic film.

We show in Fig. 3 the normalized spontaneous decay rate Γ/Γ_0 of the excited state of a molecule interacting with a single gold nanoparticle with radius $R=10$ nm, and for an emission wavelength $\lambda=500$ nm. The nanoparticle scans a rectangular region above the molecule, and the figure displays the value of Γ/Γ_0 for each position of the nanoparticle in this rectangular region. The upper panel corresponds to a nanoparticle scanning in vacuum. The lower panel corresponds to a nanoparticle coupled to the molecule through a plasmonic superlens with width $L=50$ nm. The distance between the molecule and the lower surface of the slab is $z_s=50$ nm, and the nanoparticle scans the opposite side (see the insets of Fig. 3 for a schematic view of the geometry).

If we compare the results in both panels, we observe that in the case of vacuum (upper panel), the decay-rate modification is weak (on the order of 10%) and the lateral resolution is poor (far below the nanoparticle radius). Indeed, it is known that for a nanoparticle scanning in vacuum, coupling at large distance with a nanoparticle induces weak modifications of the decay rate.[32] Substantial modifications, with a lateral resolution in the nanometer range, are reached when the distance from the molecule to the nanoparticle surface becomes comparable to the radius.[8] In the case of a nanoparticle coupled to the molecule through a plasmonic superlens (lower panel), the behavior is changed substantially. The decay-rate modification is much larger (up to a factor of 6 in the present case), and the lateral resolution is higher (we will study the lateral extent of the interaction below).[37] This first calculation demonstrates the possibility

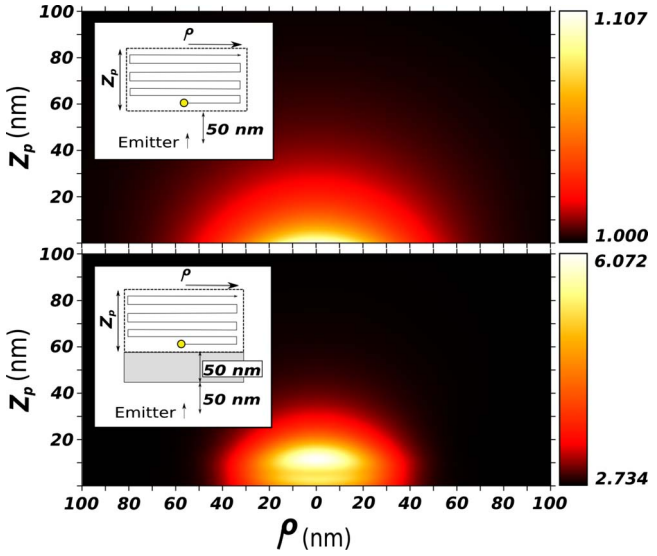

FIG. 3. (Color online) Lower panel: Normalized spontaneous decay rate of a molecule interacting with a single gold nanoparticle [radius $R=10$ nm, relative permittivity $\epsilon_p=-2.335+3.61i$ at the emission wavelength $\lambda=500$ nm (Ref. 36)] through a plasmonic superlens versus the position of the nanoparticle scanning a rectangular region in a vertical plane (see the geometry in the inset). The position of the nanoparticle is defined by the distance z_p between its surface and the slab surface and the lateral displacement ρ with respect to the position of the molecule. The transition dipole is along the z direction. Other parameters as in Fig. 2. Upper panel: same calculation without the LHM slab (molecule and nanoparticle in vacuum).

of acting on a molecule from distances in the range of a few hundreds of nanometers, with a nanometer-scale sensitivity (regarding both the lateral and the vertical displacement of the nanoparticle). A first conclusion is that plasmonic superlenses could be used to increase the range of single-molecule fluorescence control with nanoantennas.

We show in Fig. 4 the same calculation, but for a purely plasmonic slab (i.e., a nonmagnetic material with $\varepsilon=-1+0.01i$). We observe the same qualitative behavior as in the lower panel in Fig. 3. This is consistent with the fact that the coupling mechanisms are similar in the case of a plasmonic superlens and in the case of a purely metallic slab (as shown in Fig. 2, the field structure is the same). The main difference

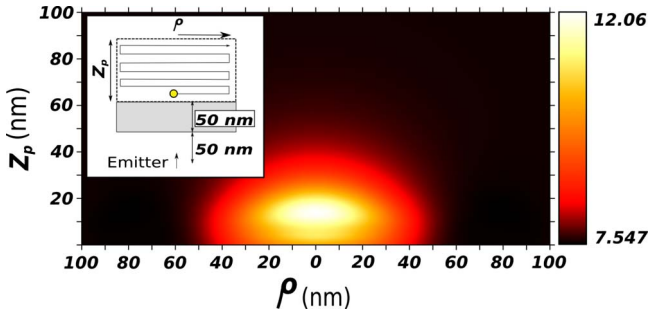

FIG. 4. (Color online) Same as Fig. 3 (lower panel) for a purely metallic slab supporting surface-plasmon polaritons, with relative permittivity $\varepsilon=-1+0.01i$ and relative permeability $\mu=1$.

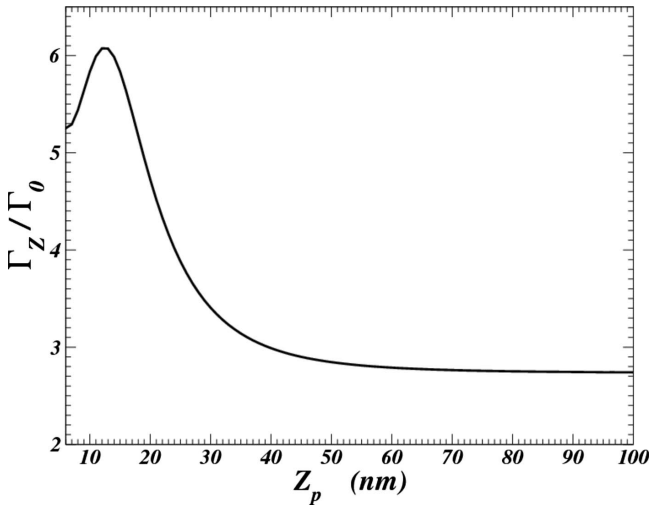

FIG. 5. Normalized decay rate of a molecule interacting with a gold nanoparticle through a plasmonic superlens versus the distance z_p between the surface of the nanoparticle and the surface of the slab. The nanoparticle scans along the z axis perpendicular to the slab surface (the lateral position corresponds to $\rho=0$ in Fig. 3, i.e., just above the molecule position). Geometrical and optical parameters as in Fig. 3.

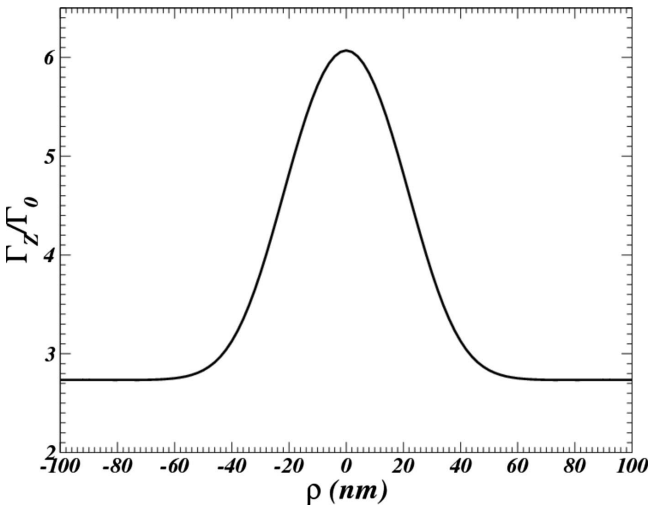

FIG. 6. Normalized decay rate of a molecule interacting with a gold nanoparticle through a plasmonic superlens versus the lateral displacement ρ between the center of the nanoparticle and the molecule location. The nanoparticle scans along a line parallel to the slab surface, with a surface-to-surface distance $z_p=11$ nm. Geometrical and optical parameters as in Fig. 3.

is that a purely metallic slab produces a worse impedance matching, reducing the contrast in the induced lifetime modifications. The purely plasmonic coupling might be much easier to perform in practice, because natural materials are available. Note that a key point is an evaluation of the fluorescence signal, and to compare the plasmonic superlens to the metallic slab in terms of fluorescence quenching. This point is under study.

IV. LOCALIZATION OF THE EMITTER

We have seen that coupling a single emitter to a metallic nanoparticle through a slab of left-handed material in the superlens regime permits substantial modifications of its dynamics. We now address the issue of the localization of the emitter from a decay-rate image obtained by scanning the nanoparticle. As far as the localization along the z direction is concerned, the field structure in Fig. 2 shows that the field on the opposite side of the slab (with respect to the emitter) decreases monotonically from the interface. Note that in terms of imaging, this means that although the high spatial frequency modes translate the subwavelength features, there is no three-dimensional subwavelength focus. In the presence of the nanoparticle, one can expect an increase in the decay-rate modification when the nanoparticle scans toward the interface. This is seen in Fig. 5, in which we show the normalized decay rate versus the distance z_p between the surface of the nanoparticle and the surface of the slab. The nanoparticle scans along the z axis perpendicular to the slab surface and above the molecule position (the curve in Fig. 5 corresponds to a vertical cut in the middle of the image in Fig. 3). We see that the decay-rate modification increases at short distance, due to an increase in the coupling strength between the emitter and the nanoparticle. In particular, there is no signature of the emitter location along the z direction. One observes a small decrease in the decay rate at very short distance (smaller than the particle radius) that is due to the nanoparticle-slab interaction.

The image in the lower panel in Fig. 3 also shows that the interaction between the molecule and the nanoparticle has a short-range extent in a plane parallel to the slab surface. In order to get a quantitative estimate of the lateral resolution, we show in Fig. 6 the normalized decay rate versus the lateral displacement ρ between the center of the nanoparticle and the molecule location (i.e., a horizontal cut of the image in Fig. 3). The distance between the molecule and the lower surface of the slab is $z_s=50$ nm (coinciding with the slab thickness), and the nanoparticle scans along a line parallel to the slab surface with a surface-to-surface distance $z_p=11$ nm. The lateral resolution can be defined as the full width at half maximum of the curve in Fig. 6, giving a resolution of roughly 50 nm in this particular case. The lateral resolution is on the order of the distance between the emitter and the slab surface (and not the full distance between the emitter and the nanoparticle). This is a feature of the coupling through a plasmonic superlens. The same behavior was found in Ref. 21.

The lateral resolution as well as the contrast in a decay-rate image depends on the distance z_s between the molecule and the slab surface. We show in Fig. 7 (upper panel) the decay-rate contrast versus the distance z_s of the molecule to the slab surface. We define the decay-rate contrast at the ratio between the maximum value and the minimum value of the decay rate in a scan image as that in Fig. 3. We observe that the contrast reaches a maximum when the emitter-slab distance z_s coincides with the slab thickness. This distance ensures the most efficient coupling between the emitter and the opposite side of the superlens. We also show in Fig. 7 (lower panel) the lateral resolution in a decay-rate image versus the

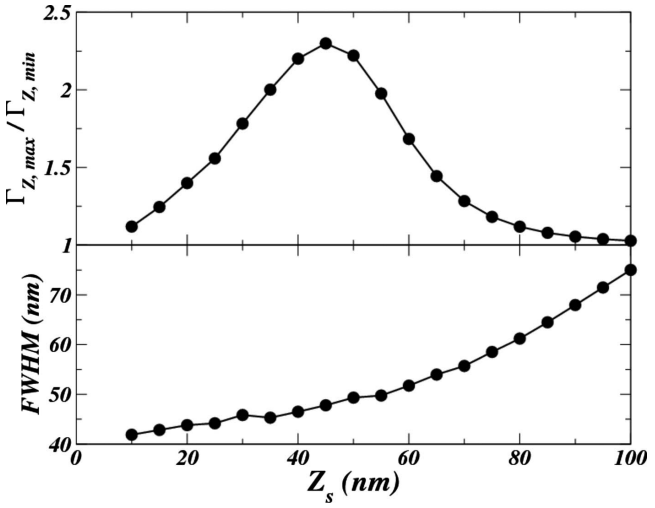

FIG. 7. Upper panel: Decay-rate contrast defined at the ratio between the maximum value and the minimum value of the decay rate in a scan image as that in Fig. 3 versus the distance z_s of the molecule to the slab surface. Other parameters as in Fig. 3. Lower panel: Lateral resolution in a decay-rate image defined as the full width at half maximum of a horizontal scan line as that in Fig. 6 versus the distance z_s of the molecule to the slab surface. Other parameters as in Fig. 6.

distance z_s. We see that the resolution decreases when the emitter-slab distance increases. This is a classical behavior in near-field optics. High resolution is provided by the evanescent modes of the slab with high spatial frequencies, which also have a short decay length along the z direction. The higher the distance z_s, the weaker the coupling to these modes. For a nanoparticle scanning at close distance from the slab surface, as in Fig. 7, the resolution is on the order of the emitter-slab distance.

V. ORIENTATION OF THE TRANSITION DIPOLE

Beyond the possibility of localizing the emitter with nanometer-scale sensitivity, the determination of the molecule orientation is a key issue. This can be achieved using nanoantennas (such as structured tips), due to the fact that the radiation pattern of the coupled system strongly depends on the orientation of the transition dipole.[11–16] We show that the coupling through a plasmonic superlens is very sensitive to the transition dipole orientation, and that the decay-rate images exhibit a clear signature of the molecule orientation. Figure 8 displays the same calculation as in Fig. 3 (lower panel), but for a transition dipole oriented along the x direction, i.e., parallel to the slab surface (in Fig. 3, the transition dipole was perpendicular to the slab surface).

We see that the decay-rate map in Fig. 8 has a different shape. The image displays two lobes, indicating the presence of two maxima of decay-rate modification when the nanoparticle scans in a plane parallel to the slab. In the case of a transition dipole perpendicular to the slab surface (lower panel in Fig. 3), only one maximum was visible at $\rho=0$, which coincides with the location of the molecule. This qualitative difference is an unambiguous signature of the

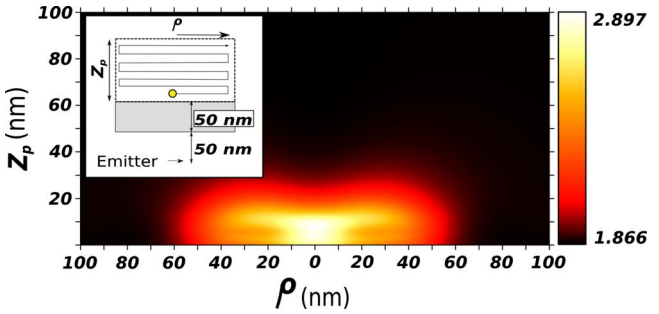

FIG. 8. (Color online) Same as Fig. 3 (lower panel) for a molecular transition dipole oriented along the x direction.

transition dipole orientation. We show in Fig. 9 a cut along a horizontal line (i.e., a curve similar to that in Fig. 6, but for a transition dipole oriented parallel to the slab surface). We clearly identify the two maxima. The contrast is large enough to discriminate between the parallel and perpendicular orientations, corresponding to a line with two maxima at each side of the molecule lateral location (Fig. 9), or one maximum at the center (Fig. 6), respectively. Also note that in terms of lateral resolution, the lateral extent of the curve in Fig. 9 is similar to that in Fig. 6. The qualitative difference between the two orientations is a consequence of the polarization dependence of the coupling to surface modes of the plasmonic superlens. At a given frequency, each mode has its own wave vector and polarization state. The coupling strength of the dipole to a given mode is strongly dependent on the relative orientation of the dipole and the direction of the electric field.

VI. INFLUENCE OF THE NANOPARTICLE MATERIAL

Before concluding, we address the question of the nanoparticle material. In practice, several metals can be used, depending on the available techniques to produce nanoparticles or tips. We show in Fig. 10 the decay-rate contrast versus the nanoparticle-slab distance z_p (upper panel) and a

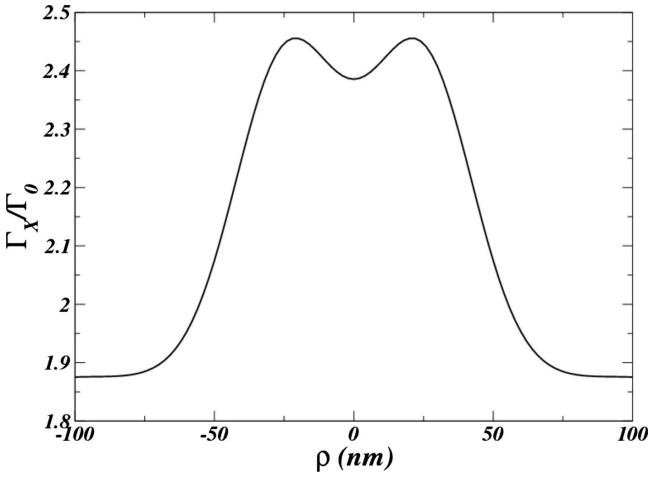

FIG. 9. Same as Fig. 6 for a molecular transition dipole oriented along the x direction. The nanoparticle scans along a line parallel to the slab surface, with a surface-to-surface distance $z_p=17$ nm.

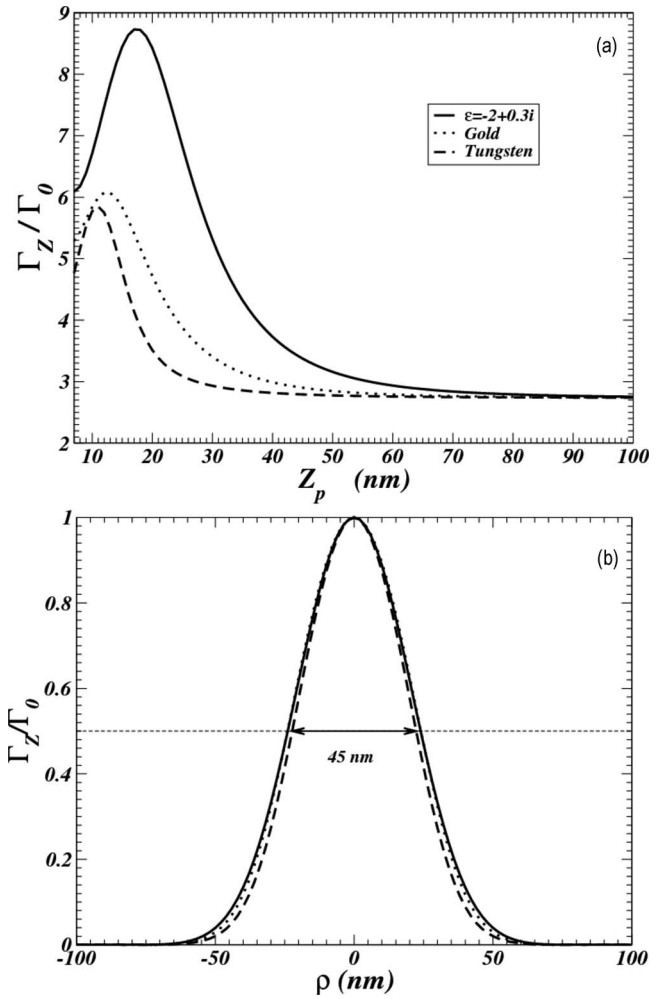

FIG. 10. Influence of the nanoparticle material. (a) Same as Fig. 5 for a nanoparticle excited at resonance with relative permittivity $\varepsilon=-2+0.3i$ at the emission wavelength $\lambda=500$ nm of the molecule (solid line), for a gold nanoparticle (dotted line) and a tungsten nanoparticle (dashed line). The radius of the nanoparticle is 10 nm in each case. (b) Decay rate of a molecule interacting with a nanoparticle through a LHM slab versus the lateral displacement ρ between the center of the nanoparticle and the molecule location taken at the surface-to-surface particle distance of maximum contrast, $z_p=16$ nm (resonant particle), $z_p=12$ nm (gold particle), and $z_p=11$ nm (tungsten particle), i.e., maxima in panel (a). The remaining parameters as in Fig. 6. The same materials as in the upper figure are considered. The three curves are normalized to their maximum value.

lateral scan versus the lateral displacement ρ, for three different cases: dipole nanoparticle at plasmon resonance (relative permittivity $\epsilon(\omega)=-2+0.3i$), gold nanoparticle, and tungsten nanoparticle. As in all calculations presented in this work, the emission wavelength is $\lambda=500$ nm. We observe that in terms of contrast and lateral resolution, the shape of the curves is independent of the nanoparticle material. This confirms that the behaviors put forward in the present study rely on the coupling through the plasmonic superlens modes, and not on a particular matching between the slab and the nanoparticle properties. Nevertheless, the contrast level strongly depends on the ability of the nanoparticle to couple efficiently to the system. As expected, a resonant nanoparticle induces larger effects, although it might be difficult in practice to design materials that produce a superlens behavior for the slab and a dipole resonance in the nanoparticle at the same frequency ω. For off-resonance nanoparticles, a comparison between gold and tungsten (a poor metal in the visible frequency range) shows that gold provides a slightly higher contrast, and a larger interaction range along the vertical direction.

VII. CONCLUSION

In summary, we have shown that a plasmonic superlens is able to couple efficiently a single molecule and a metallic nanoparticle on the range of a few hundreds of nanometers. This scheme allows the detection, the localization, and the control of the emitter dynamics with nanometer-scale sensitivity. It also permits a selective probing of the transition dipole orientation. Although the plasmonic superlens regime provides the most efficient coupling, the underlying mode structure is plasmonic in nature and is qualitatively identical to that of a purely metallic thin film excited at plasmon resonance. This means that the conclusions reached in this study remain valid qualitatively in this case, but with an efficiency that is substantially reduced. The scheme proposed in this study is appealing for applications in which the vicinity of the molecule is not directly accessible to a near-field probe, in the field of nanophotonics (e.g., emitter embedded in a solid substrate) or imaging in complex media (e.g., lifetime imaging using fluorophores in soft-matter compounds or biological media). Beyond the substantial modification of the excited state lifetime, a plasmonic superlens is expected to produce fluorescence quenching and to influence the emitter radiation pattern. These issues are under study and will be reported elsewhere.

ACKNOWLEDGMENTS

This work was supported by the EU Integrated Project "Molecular Imaging" under Contract No. LSHG-CT-2003-503259 and by the French Agence Nationale de la Recherche under Project No. CAROL BLAN06-3-134124.

*remi.carminati@espci.fr

[1] K. H. Drexhage, Sci. Am. **222**, 108 (1970).
[2] W. L. Barnes, J. Mod. Opt. **45**, 661 (1998).
[3] R. R. Chance, A. Prock, and R. Sylbey, Adv. Chem. Phys. **37**, 1 (1978).
[4] G. W. Ford and W. H. Weber, Phys. Rep. **113**, 195 (1984).
[5] R. X. Bian, R. C. Dunn, X. S. Xie, and P. T. Leung, Phys. Rev. Lett. **75**, 4772 (1995).

[6] E. J. Sanchez, L. Novotny, and X. S. Xie, Phys. Rev. Lett. **82**, 4014 (1999).
[7] J. Azoulay, A. Debarre, A. Richard, and P. Tchenio, J. Microsc. **194**, 486 (1999).
[8] P. Anger, P. Bharadwaj, and L. Novotny, Phys. Rev. Lett. **96**, 113002 (2006).
[9] B. C. Buchler, T. Kalkbrenner, C. Hettich, and V. Sandoghdar, Phys. Rev. Lett. **95**, 063003 (2005).
[10] S. Kühn, U. Hakanson, L. Rogobete, and V. Sandoghdar, Phys. Rev. Lett. **97**, 017402 (2006).
[11] E. Betzig and R. J. Chichester, Science **262**, 1422 (1993).
[12] H. Gersen, M. F. Garcia-Parajo, L. Novotny, J. A. Veerman, L. Kuipers, and N. F. van Hulst, Phys. Rev. Lett. **85**, 5312 (2000).
[13] M. Thomas, J.-J. Greffet, R. Carminati, and J. R. Arias-Gonzales, Appl. Phys. Lett. **85**, 3863 (2004).
[14] J. N. Farahani, D. W. Pohl, H.-J. Eisler, and B. Hecht, Phys. Rev. Lett. **95**, 017402 (2005).
[15] P. Mühlschlegel, H.-J. Eisler, O. J. F. Martin, B. Hecht, and D. W. Pohl, Science **308**, 1607 (2005); J.-J. Greffet, *ibid.* **308**, 1561 (2005).
[16] T. H. Taminiau, F. D. Stefani, F. B. Segerink, and N. F. van Hulst, Nat. Photonics **2**, 234 (2008).
[17] P. Andrew and W. L. Barnes, Science **306**, 1002 (2004).
[18] F. D. Stefani, K. Vasilev, N. Bocchio, N. Stoyanova, and M. Kreiter, Phys. Rev. Lett. **94**, 023005 (2005).
[19] N. Fang, H. Lee, C. Sun, and X. Zhang, Science **308**, 534 (2005).
[20] D. O. S. Melville and R. J. Blaikie, Opt. Express **13**, 2127 (2005).
[21] T. Taubner, D. Korobkin, Y. Urzhumov, G. Schvets, and R. Hillenbrand, Science **313**, 1595 (2006).
[22] J. B. Pendry, Phys. Rev. Lett. **85**, 3966 (2000).
[23] D. R. Smith, J. B. Pendry, and M. C. K. Wiltshire, Science **305**, 788 (2004).
[24] R. A. Shelby, D. R. Smith, and S. Schultz, Science **292**, 77 (2001).
[25] V. M. Shalaev, W. Cai, U. K. Chettiar, H.-K. Yuan, A. K. Sarychev, V. P. Drachev, and A. V. Kildishev, Opt. Lett. **30**, 3356 (2005).
[26] S. Zhang, W. Fan, N. C. Panoiu, K. J. Malloy, R. M. Osgood, and S. R. J. Brueck, Phys. Rev. Lett. **95**, 137404 (2005).
[27] C. M. Soukoulis, S. Linden, and M. Wegener, Science **315**, 47 (2007).
[28] M. Nieto-Vesperinas, J. Opt. Soc. Am. A **21**, 491 (2004).
[29] J. M. Wylie and J. E. Sipe, Phys. Rev. A **30**, 1185 (1984).
[30] J. E. Sipe, J. Opt. Soc. Am. B **4**, 481 (1987).
[31] B. T. Draine, Astrophys. J. **333**, 848 (1988).
[32] R. Carminati, J.-J. Greffet, C. Henkel, and J. M. Vigoureux, Opt. Commun. **261**, 368 (2006).
[33] A. Rahmani, P. C. Chaumet, F. de Fornel, and C. Girard, Phys. Rev. A **56**, 3245 (1997).
[34] L. S. Froufe-Pérez, R. Carminati, and J. J. Sáenz, Phys. Rev. A **76**, 013835 (2007).
[35] D. Sarid, Phys. Rev. Lett. **47**, 1927 (1981).
[36] E. W. Palik, *Handbook of Optical Constants of Solids* (Academic, San Diego, 1985).
[37] Although not shown for the sake of brevity, we have verified that in the case of a perfect lens (i.e., a slab of nonabsorbing material with both $\epsilon(\omega)=-1$ and $\mu(\omega)=-1$), the molecule couples perfectly with the focus on the other side of the slab. When the nanoparticle approaches the focus, the decay rate changes as if the emitter was placed at the focus. This is a direct consequence of the perfect focusing described in Ref. 22. This situation is never reached in the case of absorbing materials, since the coupling mechanism is different (as described in Fig. 2).